Development and Testing of a Frozen Soil Parameterization for Cold Region Studies

XIA ZHANG

Institute of Atmospheric Physics, Chinese Academy of Science, Beijing, China

SHUFEN SUN

State Key Laboratory of Numerical Modeling for Atmospheric Sciences and Geophysical Fluid Dynamics, Institute of Atmospheric Physics, Chinese Academy of Science, Beijing, China

YONGKANG XUE

Departments of Geography and Atmospheric and Oceanic Sciences, University of California, Los Angeles, Los Angeles, California

(Manuscript received 1 May 2006, in final form 15 December 2006)

ABSTRACT

Proper simulation of soil freezing and thawing processes is an important issue in cold region climate studies. This paper reports on a frozen soil parameterization scheme for cold region studies that includes water flow and heat transfer in soil with water phase change. The mixed-form Richards' equation is adopted to describe soil water flow affected by thermal processes in frozen soil. In addition, both liquid water and ice content have been taken into account in the frozen soil hydrologic and thermal property parameterization. To solve the complex nonlinear equation set and to ensure water conservation during simulation of complex phase change processes, efficient computational procedures have been designed and a new modified Picard iteration scheme is extended to solve the mixed-form Richards' equation with phase change. The frozen soil model was evaluated using observational data from the field station at Rosemount, Minnesota, and the Tibet D66 site. The results show that the model is capable of providing good simulations of the evolution of temperature and liquid water content in frozen soil. Comparisons of simulation results from sensitivity studies indicate that there is a maximum difference of about 50 W m^{-2} in sensible and ground heat fluxes with and without the inclusion of the effect of ice content on matric potential and that using the exponential relationship between hydraulic conductivity and ice content produces realistic results.

1. Introduction

The area of frozen soil, including permafrost and seasonal frost, accounts for about 20% of the earth's land area (Peixoto and Oort 1992). Frozen soil processes in cold regions play an important role in climate change and weather forecasting (Mölders and Walsh 2004; Poutou et al. 2004; Viterbo et al. 1999). For example, the freeze–thaw cycle modulates the change of both soil temperature and the overlying air temperature due to release or absorption of latent heat during freezing and thawing processes. These processes change the thermal and hydraulic properties of soil, such as volumetric heat capacity, thermal conductivity, and hydraulic conductivity, because volumetric heat capacity of ice is half that of liquid water and thermal conductivity of ice is about 4 times that of liquid water. Changes in these properties definitely affect the surface water and energy balances.

Studies have shown that proper frozen soil schemes help improve land surface and climate model simulations (e.g., Cox et al. 1999; Viterbo et al. 1999; Smirnova et al. 2000; Poutou et al. 2004). For example, comparisons of results from the Project for Intercomparison of Land Surface Parameterization Schemes Phase 2(d) [PILPS 2(d)] have shown that the models with an explicit frozen soil scheme give a much more realistic soil temperature simulation during winter than those without a frozen scheme (Luo et al. 2003). A frozen soil model with realistic simulation of soil temperature, moisture content, and ice content also improves the

Corresponding author address: ShuFen Sun, LASG, Institute of Atmospheric Physics, Chinese Academy of Science, Beijing 100029, China.
E-mail: ssf@lasg.iap.ac.cn

DOI: 10.1175/JHM605.1

TABLE 1. Comparison of the existing frozen soil parameterization schemes.

Matric potential	$\psi = \psi(\theta_l)$		Slater et al. 1998; Koren et al. 1999; Cox et al. 1999; Cherkauer and Lettenmaier 1999; Warrach et al. 2001; Mölders et al. 2003; Dai et al. 2003
	$\psi = \psi(\theta_l, \theta_i)$		Koren et al. 1999; Smirnova et al. 2000; this paper
Hydraulic conductivity	$K = K(\theta_l)$		Slater et al. 1998; Cox et al. 1999; Koren et al. 1999; Warrach et al. 2001; Mölders et al. 2003; Dai et al. 2003
	$K = K(\theta_l, \theta_i)$	Linear	Smirnova et al. 2000
		Exponential	This paper
Determination of ice content	Heat available		Slater et al. 1998; Takata and Kimoto 2000; Dai et al. 2003
	The freezing point depression equation		Cherkauer and Lettenmaier 1999; Cox et al. 1999; Koren et al. 1999; Smirnova et al. 2000; Warrach et al. 2001; Mölders et al. 2003; Niu and Yang 2006; this paper
	Empirical equation		Pauwels and Wood 1999; Li and Koike 2003
Water balance equation	Water and vapor flow		Mölders et al. 2003; this paper
	Water flow only		Most of the frozen soil schemes

climate model's ability to simulate greenhouse gas exchange processes in cold regions (Mikan et al. 2002).

In recent years, efforts have been made to develop frozen soil parameterizations in land surface schemes for atmospheric models. The parameterization for frozen soil processes can generally be divided into two categories according to the methodology defining the freezing point in the soil. The schemes in the first category are based on a fixed freezing point (273.16 K), and the proportion of water changing to ice is determined based on the amount of heat energy available for phase change processes (e.g., Slater et al. 1998; Takata and Kimoto 2000; Dai et al. 2003). The schemes in the second category have an unfixed freezing point and a continuous freezing process. The partition of total water into liquid water and ice is determined based on the freezing-point depression equation, in which soil matric potential is a function of temperature (e.g., Cherkauer and Lettenmaier 1999; Cox et al. 1999; Smirnova et al. 2000; Koren et al. 1999; Warrach et al. 2001; Mölders et al. 2003; Niu and Yang 2006), or on empirical equations from laboratory observations (Pauwels and Wood 1999; Li and Koike 2003) (Table 1).

The schemes in category 1 simplify the treatment of the physical processes of freezing and thawing in the soil. In reality, however, ice rarely forms at 0°C in a soil medium and some amount of unfrozen water still exists at temperatures lower than 0°C. In category 2, most schemes assume that the relationship between the matric potential and unfrozen water content in unfrozen soil can be extended to frozen soil as done in Miller (1980), except for Koren et al. (1999) and Smirnova et al. (2000), who have taken the effect of ice content on soil matric potential into account. Findings from laboratory experiments (Farouki 1986; Xu et al. 2001) have shown that unfrozen water exists not only on the surface of soil particles but also among ice crystals. Therefore ice content influences the matric potential in frozen soil. Furthermore, according to experimental data, the presence of ice may significantly decrease hydraulic conductivity of a porous medium (Jame and Norum 1980). Numerical experiments also show that without consideration of impedance of the ice content to the water flow, too much water accumulates near the freezing front, which is inconsistent with observational data (Harlan 1973; Taylor and Luthin 1978). However, only the scheme from Smirnova et al. (2000) has explicitly taken into account this blocking effect with a linear relationship between ice content and hydraulic conductivity. In this paper, an exponential relationship is applied and will be discussed in section 4.

According to the freezing-point depression equation, matric potential in frozen soil is also a function of temperature (Williams 1967; Cary and Mayland 1972; Fuchs et al. 1978). Consequently, soil temperature, ice content, and unfrozen water content are in a delicate equilibrium state. A slight change in energy and mass balances will disturb the equilibrium of the three water phases in the soil, which in turn causes the release or absorption of latent heat and then a change in soil temperature. These changes would further alter the heat and water fluxes. All of these interactive effects, through the coupling of thermal and hydrological processes, are more prominent in the frozen zone with abrupt phase transition. However, only a few schemes for frozen soil deal with these cross effects (Flerchinger and Saxton 1989; Mölders et al. 2003). Moreover, most schemes in category 2 use some assumptions for easy-to-obtain approximate numerical solutions for soil water and energy balance equations with phase change. In this paper, equations are solved by the iteration scheme, which obtains solutions of soil temperature and matric potential satisfying the freezing-point depression equation accurately.

In this study, a 1D frozen soil parameterization coupling the thermal and hydrological processes is developed, which accounts for the effects of ice content on matric potential and on hydraulic conductivity. A modified Picard iteration method is extended to solve the water balance differential equation with phase change, and an efficient computational procedure is designed for the nonlinearity and complexity of frozen soil physics. Datasets from a plot-scale field experiment at Rosemount, Minnesota, which were widely used for model evaluation (Cherkauer and Lettenmaier 1999; Koren et al. 1999; Pauwels and Wood 1999; Warrach et al. 2001), and from the Global Energy and Water Cycle Experiment (GEWEX) Asian Monsoon Experiment (GAME)/Tibet D66 site are used to test the model. Section 2 describes the frozen soil parameterization. Field data for evaluation are presented in section 3. Simulation results and conclusions are given in sections 4 and 5, respectively.

2. Model description

a. Governing equations

1) WATER BALANCE EQUATION AND PARAMETERIZATIONS

Liquid and vapor movement, as well as phase change, affects soil moisture in a frozen or unfrozen soil zone. Liquid water flow in frozen soil is considered to be analogous to that in unfrozen soil and can still be described by Darcy's law (Harlan 1973). Vapor flow in the water balance is not unimportant, especially when soil moisture can be transferred only through vapor flow in an unsaturated frozen soil during a long wintertime (Mölders et al. 2003). A generalized mixed-form Richards' equation is used to describe the vertical profile of soil moisture in a frozen or unfrozen soil zone by combining Darcy's law and the conservation of mass as (Flerchinger and Saxton 1989)

$$\frac{\partial \theta_l}{\partial t} = -\frac{\rho_i}{\rho_l}\frac{\partial \theta_i}{\partial t} - \frac{\partial}{\partial Z}\left(-K\frac{\partial \psi}{\partial Z} + K\right) + \frac{1}{\rho_l}\frac{\partial}{\partial Z}\left(D_{\mathrm{TV}}\frac{\partial T}{\partial Z} + D_{\psi \mathrm{V}}\frac{\partial \psi}{\partial Z}\right), \quad (1)$$

where θ_l and θ_i are volumetric liquid water content and ice content ($m^3\ m^{-3}$), t is the time (s), ρ_l and ρ_i are the density of liquid water and ice, respectively ($kg\ m^{-3}$), Z is the soil depth (m), K is soil hydraulic conductivity ($m\ s^{-1}$), T is soil temperature (°C), ψ is soil matric potential (m), D_{TV} is thermal vapor diffusivity ($kg\ m^{-2}\ s^{-1}$) due to temperature gradient, and $D_{\psi \mathrm{V}}$ is the vapor diffusivity ($kg\ m^{-1}\ °C^{-1}\ s^{-1}$) due to soil matric potential gradient. The driving force of the liquid water movement in frozen soil is not simply expressed by volumetric water content gradient because matric potential also is affected by ice content. Therefore, we selected the mixed form of Richards' equation. Equation (1) has merit in that its numerical scheme possesses the conservation property (Celia et al. 1990).

In unsaturated frozen soil, when ice is presented, soil water potential remains in equilibrium with the vapor pressure over pure ice (Flerchinger and Saxton 1989). Based on this thermodynamic relationship and the Clausius–Clapeyron equation, the relationship of soil matric potential and temperature in frozen soil, referred to as the freezing-point depression equation, can be derived. Many frozen soil parameterizations have used the freezing-point depression equation given by Cary and Mayland (1972), with soil water osmotic potential neglected:

$$\psi = \frac{L_{\mathrm{il}} T}{g(T + T_0)}, \quad (2)$$

where L_{il} is the latent heat of fusion ($J\ kg^{-1}$), g is the acceleration of gravity ($m\ s^{-2}$), and T_0 is the freezing point of free water (273.16 K). However, based on our derivation, the freezing-point depression equation should be given by

$$\psi = \frac{L_{\mathrm{il}} T}{g T_0}, \quad (3)$$

which is the same as that of Williams (1967). Since T (°C) is much smaller than T_0 (K) in Eq. (2), the difference in matric potential between using Eqs. (3) and (2) would not be very large. For instance, when temperature is at −10°C, matric potential from Eq. (3) is 3.6% larger than that from Eq. (2). However, the simple relationship in Eq. (3) makes it easy to determine soil freezing temperature and to solve equations for the coupled thermal and hydrological processes.

The matric potential in frozen soil should also be a function of both liquid water and ice content in soil (Farouki 1986; Xu et al. 2001). Based on the constitutive relationship between matric potential and liquid moisture content in unfrozen soil (Clapp and Hornberger 1978), a parameterization has been developed to consider the effect of ice on the matric potential (Kulik 1978; Koren et al. 1999):

$$\psi = \psi_0\left(\frac{\theta_l}{\theta_s}\right)^{-b}(1 + C_k\theta_i)^2, \quad (4)$$

where ψ_0 is saturated matric potential (m), θ_s is saturated water content ($m^3\ m^{-3}$), b is the Clapp–Horn-

berger constant, and C_k represents the effect of soil specific surface on matric potential due to the presence of ice. Kulik reported an average value of about 8 for C_k.

From Eqs. (3) and (4), we can obtain

$$T = (\psi_0 g T_0 / L_{il})(\theta_l/\theta_s)^{-b}(1 + C_k\theta_i)^2. \quad (5)$$

With a given set of liquid water content and ice content, when temperature rises higher than the value determined by Eq. (5), soil ice begins to thaw. Otherwise, liquid water freezing continues.

Unsaturated hydraulic conductivity K in frozen soil is an important physical parameter. Due to the impedance of the ice to liquid moisture flow, hydraulic conductivity is a function of both liquid water content and ice content. In this frozen soil parameterization, the Clapp–Hornberger relation for K in unfrozen soil is modified following Jame and Norum (1980):

$$K = 10^{-E_i\theta_i} K_{\text{sat}} \left(\frac{\theta_l}{\theta_s}\right)^{3+2b}, \quad (6)$$

where K_{sat} is saturated hydraulic conductivity of unfrozen soil (m s^{-1}) and E_i is a dimensionless empirical constant as a factor of impedance from ice and given by an empirical equation (Shoop and Bigl 1997):

$$E_i = \frac{5}{4}(K_{\text{sat}} - 3)^2 + 6, \quad (7)$$

where K_{sat} is in centimeters per hour. Equation (6) as an empirical relationship is based on experimental observations of an exponential decline in hydraulic conductivity associated with ice in soil pores and is used by some researchers (Taylor and Luthin 1978; Lundin 1990; Shoop and Bigl 1997; Stähli et al. 1999). After comparing the results from a number of empirical mathematical formulations, Guymon et al. (1993) found that using Eq. (7) yielded the best results.

2) Heat balance equation

The heat balance equation with water phase change in soil used in this model can be written as (Harlan 1973)

$$\frac{\partial}{\partial t}(C_s T) = \frac{\partial}{\partial Z}\left(\lambda \frac{\partial T}{\partial Z}\right) + L_{il}\rho_i \frac{\partial \theta_i}{\partial t}, \quad (8)$$

where C_s is the effective volumetric heat capacity of the soil ($\text{J m}^{-3}\ ^\circ\text{C}^{-1}$), and λ is the thermal conductivity ($\text{W m}^{-1}\ ^\circ\text{C}^{-1}$) and is parameterized by the modified method of Johanson (1975) (Farouki 1981; Peters-Lidard et al. 1998), which is generally considered superior to all other methods as indicated by Farouki (1981). In this equation, the contribution of latent heat associated with vapor movement is neglected because it is two orders of magnitude smaller than heat conduction (Sun et al. 2003).

3) Approaches of numerical solutions

The equation set [(1), (4), (5), (8)] is a closed system for four unknown variables: θ_l, ψ, θ_i, and T. To simplify computational processes, many frozen soil schemes avoid solving the full set of equations and impose some constraints to make the solutions easy to obtain (e.g., Koren et al. 1999). However, in this type of approach, numerical solutions of soil temperature and matric potential do not satisfy the freezing-point depression equation. In this study, we try to accurately solve this full set of highly nonlinear equations. Equations (1) and (8) are discretized using fully implicit difference approximation, and iteration procedures are used to solve the discrete equation set for mass and energy conservation. The Newton iterative numerical scheme is used for Eq. (8). The modified Picard iteration algorithm, proposed by Celia et al. (1990), is extended to solve Eq. (1) but with consideration of phase changes in our model. The Picard iteration method is generally believed to be superior to the Newton iteration method in computational efficiency and conservation for the mixed-form Richards' equation (Huang et al. 1998). Hansson et al. (2004) applied this iteration scheme for the mixed-form Richards' equation and found that it performs very well, but in their study, no relationship between ice and matric potential is included.

In this study, efficient computational procedures are designed to solve equations while ensuring quick convergence of the solutions. The fully implicit difference approximation to Eq. (1) coupled with the Picard iteration scheme is called the Picard iteration difference scheme hereafter. An approach similar to the one used by Celia et al. (1990) is used to eliminate unknown $\theta_l^{k+1,m+1}$ at the new time level and the last iteration from the Picard iteration difference equation, where superscript k indicates the time level and superscript m the iteration number. The numerical schemes and computational procedure are presented as follows. Because θ_l in Eq. (4) can be considered a function of ψ and θ_i, $\theta_l^{k+1,m+1}$ can be given by the first-order approximation

$$\theta_l^{k+1,m+1} = \theta_l^{k+1,m} + C_w^{k+1,m}(\psi^{k+1,m+1} - \psi^{k+1,m}) + C_i^{k+1,m}(\theta_i^{k+1,m+1} - \theta_i^{k+1,m}), \quad (9)$$

where $C_w^{k+1,m} = (\partial\theta_l/\partial\psi)^{k+1,m}$ and $C_i^{k+1,m} = (\partial\theta_l/\partial\theta_i)^{k+1,m}$ at the new time level and the previous iteration. Thus, the difference term of θ_l with respect to time Δt can be approximated by

$$\frac{\Delta\theta_l}{\Delta t} = \frac{\theta_l^{k+1,m+1} - \theta_l^k}{\Delta t} = \frac{\theta_l^{k+1,m+1} - \theta_l^{k+1,m} + \theta_l^{k+1,m} - \theta_l^k}{\Delta t}$$

$$= \frac{C_w^{k+1,m}(\psi^{k+1,m+1} - \psi^{k+1,m}) + C_i^{k+1,m}(\theta_i^{k+1,m+1} - \theta_i^{k+1,m})}{\Delta t} + \frac{\theta_l^{k+1,m} - \theta_l^k}{\Delta t}. \quad (10)$$

Equation (10) is substituted into the Picard iteration difference scheme of Eq. (1), and then we have a new equation referred to as Eq. (1*), with the three unknown variables $\psi^{k+1,m+1}$, $\theta_i^{k+1,m+1}$, and $T^{k+1,m+1}$ at the new time level and the last iteration level. To obtain the four variables (θ_l, ψ, θ_i, and T), the four equations are solved successively at an iteration level. The computation procedure is as follows: 1) at new time-level $k + 1$, known θ_i^k, T^k or $\theta_i^{k+1,m}$, $T^{k+1,m}$ are assigned to the unknown ice content $\theta_i^{k+1,1}$, $T^{k+1,1}$ or $\theta_i^{k+1,m+1}$, $T^{k+1,m+1}$, respectively, and then Eq. (1*) is solved to obtain $\psi^{k+1,m+1}$; 2) using Eq. (4), $\theta_l^{k+1,m+1}$ can be obtained; 3) with known $\theta_l^{k+1,m+1}$ and $\theta_i^{k+1,m+1}$, the Newton iteration scheme for the implicit difference form of Eq. (8) is solved to obtain $T^{k+1,m+1}$; and 4) update $\theta_i^{k+1,m+1}$ using Eq. (11).

In principle, after solving for $T^{k+1,m+1}$ and $\theta_l^{k+1,m+1}$, $\theta_i^{k+1,m+1}$ could be obtained from Eq. (5). However, Eq. (5) shows high nonlinearity among temperature, liquid moisture content, and ice content in frozen soil physics. A slight phase change could produce relatively large variations in soil temperature due to release or absorption of latent heat, which makes the convergence of the solutions difficult. Therefore, we develop a numerical scheme to estimate $\theta_i^{k+1,m+1}$:

$$\theta_i^{k+1,m+1} = \theta_i^{k+1,m} + \omega(T^{k+1,m+1} - T^{*k+1,m+1})/\gamma, \quad (11)$$

where ω is a relaxation factor and γ is the unit conversion factor (K) $[C_t/(L_{il}\rho_i)]$. Here $T^{*k+1,m+1}$ is calculated according to Eq. (5) with the known $\theta_l^{k+1,m+1}$ and $\theta_i^{k+1,m+1}$ that are used in step 1. This estimation for temperature is based on the fact that soil temperature change is small during a phase change. The variable $\theta_i^{k+1,m+1}$ from Eq. (11) avoids numerical oscillations of calculated temperature due to the release or absorption of latent heat from phase change. We can accelerate the convergence of iteration by selecting a suitable parameter $\omega = 0.5$ in the iteration procedure.

Iteration starts again at step 1 until the convergences of the solutions for θ_i, θ_l, and T are reached. To save computational time, the number of iterations at each time step is limited to less than 10 times. Our experiments show that the methodology described in this paper ensures that adequate convergence is reached even when drastic phase change occurs.

b. Boundary conditions

The upper boundary condition for Eq. (1) on a bare soil surface is given by the vertical moisture flux $q_{s\theta}$ (m s^{-1}) and is defined as

$$q_{s\theta} = U_p - E - R_s, \quad (12)$$

where E is evaporation rate (m s^{-1}), U_p is rainfall rate (m s^{-1}) on the soil surface, and R_s is surface runoff. If there is snow falling, the snow will create a snow cover over bare soil and a snow cover model, such as the snow–atmosphere–soil transfer model (SAST) developed by Sun et al. (1999), is needed to couple with this frozen soil model.

The upper boundary condition for Eq. (8) on a bare soil surface is given by the ground heat flux G (W m^{-2}) and is defined as

$$G = \rho_l C_l T_p(U_p - R_s) + R_n - H_s - LE^*, \quad (13)$$

where T_p is the temperature of rain (°C), R_n is net radiation flux (W m^{-2}), H_s is sensible heat flux (W m^{-2}), and LE^* is latent heat flux (W m^{-2}). The term $\rho_l C_l T_p(U_p - R_s)$ in Eq. (13) is heat flux brought by the rain infiltration (W m^{-2}). The sensible and latent heat fluxes are calculated using the Monin–Obukhov theory and will not be discussed in detail in this paper.

For the lower boundary conditions, the gradients of temperature and matric potential are both equal to zero. However, the gravitational flow still exists for water flux at the lower boundary.

TABLE 2. Parameters for the Rosemount station and D66 site.

	Rosemount station	D66 site
Soil porosity	0.4676	0.3857
Saturation soil suction (m)	−0.4540	−0.0639
Saturation conductivity (m s^{-1})	5×10^{-7}	2×10^{-6}, 1×10^{-7}
Clapp–Hornberger parameter b	4.98	3.86
Roughness length (m)	0.045	0.002
Albedo	0.16–0.24*	0.2

* Denotes that albedo is calculated based on observational downward and upward solar radiation fluxes. However, the value of albedo is not used in the model simulation.

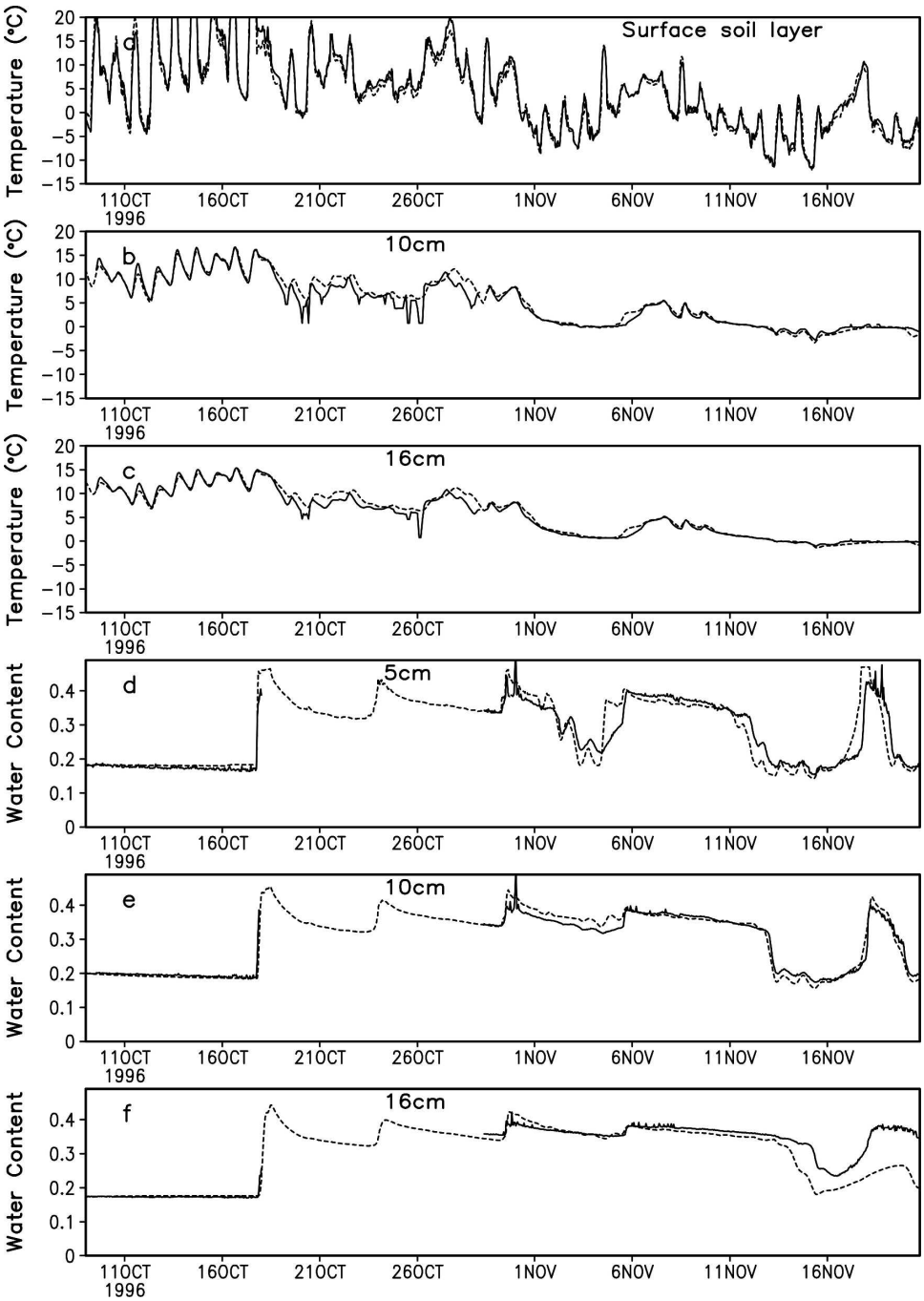

FIG. 1. Observed (solid lines) and simulated (dashed lines) (a)–(c) soil temperature (°C) and (d)–(f) volumetric liquid water content ($m^3\ m^{-3}$) at the indicated depths at Rosemount station from 9 Oct to 21 Nov 1996.

c. Model configuration and experimental setting

The frozen soil model is composed of 10 layers. Analysis of computational stability in numerical tests has shown that the topsoil layer thickness of 2 cm is proper for a time step of 15–30 min. With respect to the arrangement of the layer thickness, we set high vertical resolution for the top 50-cm soil layers and coarse resolution for the deep soil layers. In the simulation study discussed in the next sections, we set the measurement depths as the middle point of the layers for easy comparison with observations. The bottom boundary posi-

TABLE 3. Statistical errors of simulated temperature (°C) and volumetric liquid water content ($m^3\ m^{-3}$) at different depths from Rosemount station.

	Temperature		Water content	
	MBE	RMSE	MBE	RMSE
Surface	−0.118	1.038		
5 cm			0.000	0.044
10 cm	0.114	0.571	0.004	0.019
16 cm	0.212	0.479	−0.018	0.037
20 cm	0.096	0.344	0.019	0.040
31 cm	0.079	0.360	−0.005	0.024
48 cm	−0.102	0.441	0.035	0.047
65 cm	−0.682	0.770	0.011	0.038
100 cm	0.350	0.428	0.002	0.003

TABLE 4. Statistical errors of simulated temperature (°C) and volumetric liquid water content ($m^3\ m^{-3}$) at different depths from the D66 site.

	Temperature		Water content	
	MBE	RMSE	MBE	RMSE
Surface	−0.023	2.181		
4 cm	−0.034	1.269	−0.031	0.048
20 cm	0.111	0.479	−0.017	0.026
40 cm	0.147	0.268		
60 cm	0.184	0.284	−0.009	0.014
80 cm	0.176	0.293		
100 cm	0.232	0.325	0.003	0.004
130 cm	0.293	0.370		
160 cm	0.123	0.180	0.001	0.0012
200 cm	0.011	0.076		
263 cm	−0.087	0.099		

tion is placed at a depth of 6 m. Initial soil water content and temperature profiles were estimated by interpolation from the measured values. Simulations were run at a time step of 30 min.

3. Field data for model evaluation

Because this parameterization scheme does not include physical processes in vegetation and snow cover, for model evaluation, the numerical simulation is confined to the period when soil freezing/thawing processes occur without vegetation and snow cover. Two observational datasets are used to evaluate the model.

a. Rosemount field experiment data

The Rosemount station is located approximately 30 km south of St. Paul, Minnesota (44°43′N, 93°05′W; 290-m elevation). All measurements were made at the center of a relatively flat, 17-ha farm field. Available data from the University of Minnesota Rosemount Agriculture Experiment Station include meteorological data and soil temperature and liquid water profiles (Koren et al. 1999; Warrach et al. 2001). The soil is silt loam and the soil parameters used in this simulation are listed in Table 2 (Beringer et al. 2001; Clapp and Hornberger 1978), where the saturated conductivity is calibrated based on Clapp and Hornberger (1978).

b. Tibet D66 site data

The D66 site is located in the northern, arid area of the Tibetan Plateau (35°31′N, 93°47′E; 4560-m elevation). Its annual precipitation is very little according to observational data from the nearest meteorological station (M. X. Yang 2003, personal communication). Soil temperature and liquid water content were observed at different depths of sparse grassland (Yang et al. 2003). An automatic weather station measured the meteorological data without precipitation, upward solar radiation, and downward longwave radiation. At the D66 site the soil is loam sandy, and the soil parameters in this simulation are listed in Table 2 (Beringer et al. 2001; Clapp and Hornberger 1978). Taking the soil vertical heterogeneity (information from the site pictures; not shown) into account, two saturated hydraulic conductivities for the shallow and deep soil portions are used for this simulation.

4. Simulation results and discussion

a. Evaluation of the model simulation

1) ROSEMOUNT STATION

The period from 9 October to 21 November, when the soil has frozen without overlying snow cover, is selected for model evaluation. Figure 1 displays half-hourly observed and simulated soil temperature and volumetric liquid water content at different depths. The errors of simulated soil temperature and volumetric liquid water content at all observational depths for the period having observational data are shown in Table 3 (observational water contents at depths 31–65 cm show unrealistic oscillation during precipitation periods). The mean bias errors (MBEs) for soil temperature are small at various soil layers, less than 0.3°C for most layers, and the root-mean-square errors (RMSEs) are less than 0.5°C for most layers. Only the surface layer has the relative larger RMSE of 1.038°C. It can be seen that simulated soil temperatures are in good agreement with observed values (Table 3). Simulated soil liquid water contents match the observed values very well with the MBE being less than 0.03 (Table 3). During this simulation period there were two frost events. The

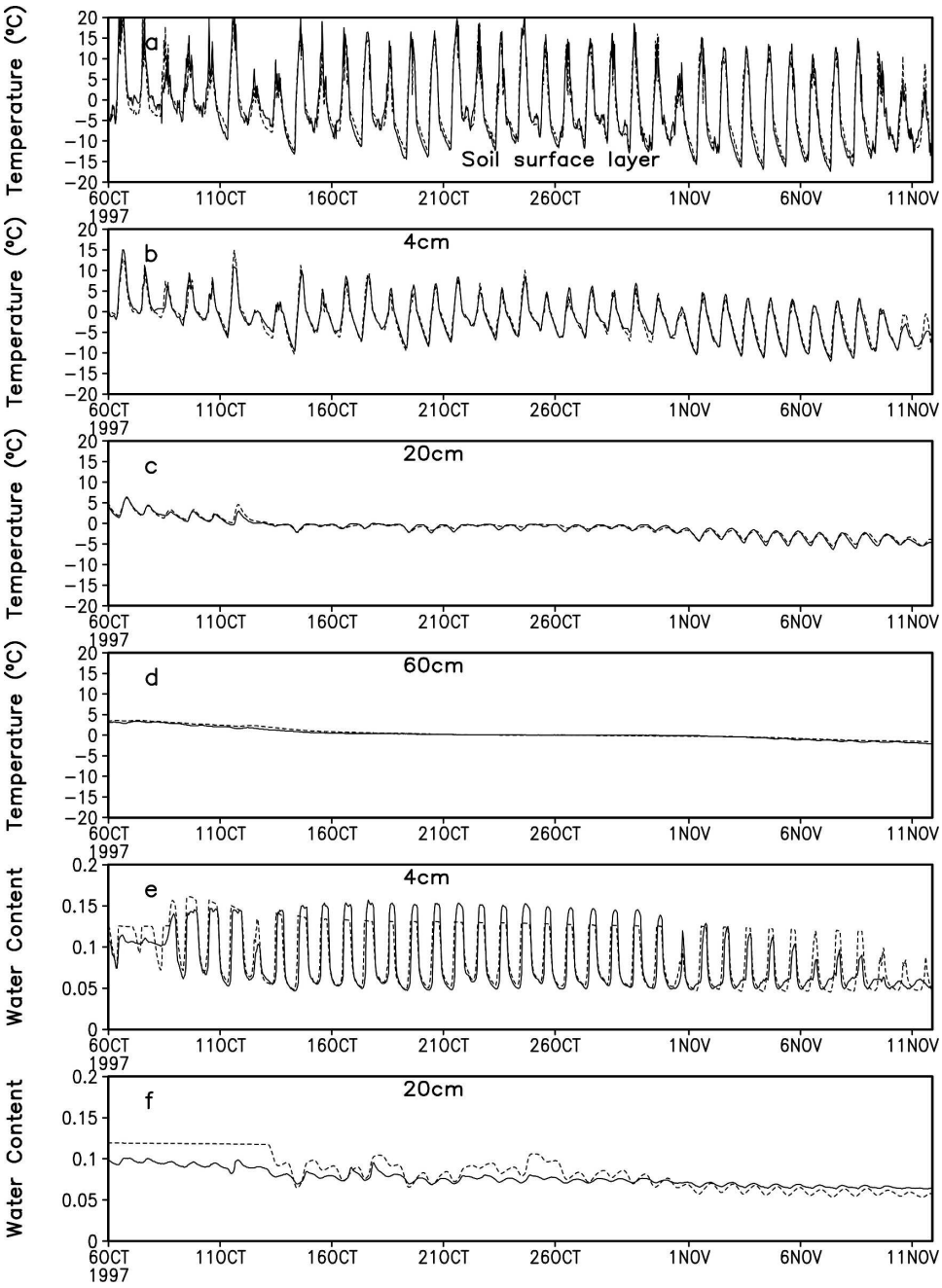

FIG. 2. Observed (solid lines) and simulated (dashed lines) (a)–(d) soil temperature (°C) and (e), (f) volumetric liquid water content ($m^3\ m^{-3}$) at the indicated depth at the Tibet D66 site from 6 Oct to 12 Nov 1997.

freezing and thawing processes during these two events are well simulated except at the depth of 16 cm during 15–21 November (Figs. 1d,e). It seems that underestimation of simulated soil temperatures at the depth of 16 cm leads to a quicker decrease/lesser increase in volumetric liquid water content owing to earlier soil freezing/delayed thawing than observed.

2) TIBET D66 SITE

We chose the period from 6 October 6 to 12 November 1997 to evaluate the model simulation when the penetration of freezing and thawing processes to the deep soil layers was well represented. Table 4 shows the errors of simulated soil temperature and liquid water

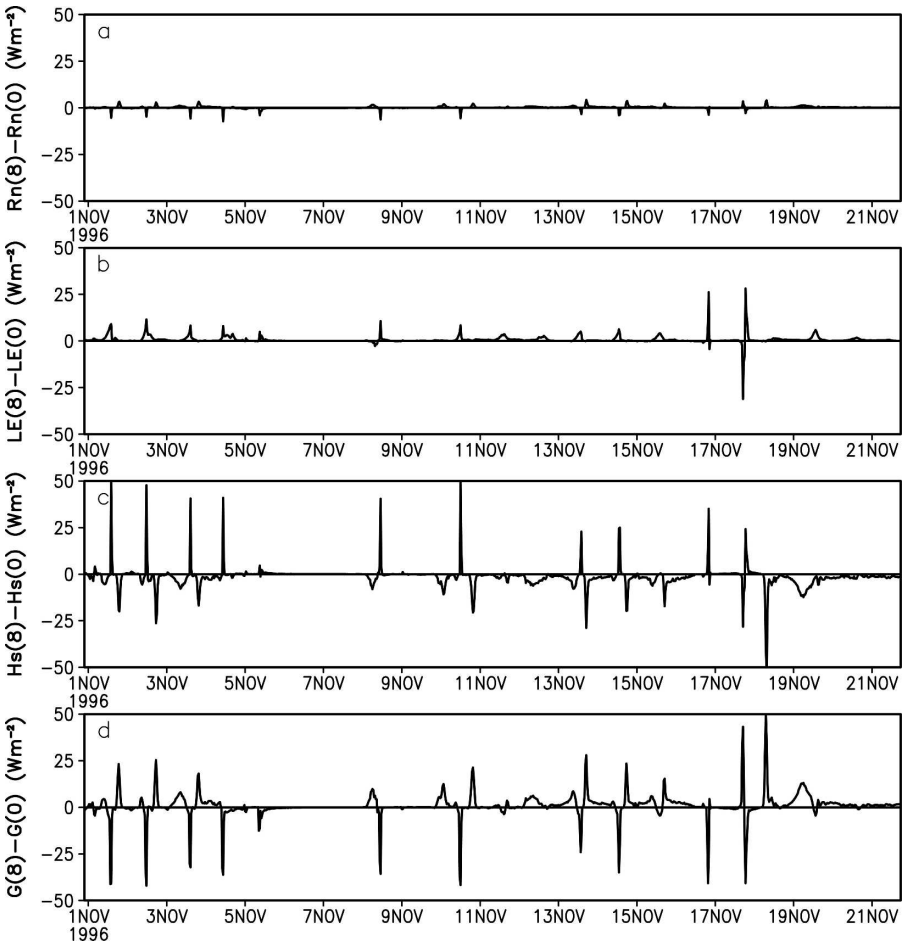

FIG. 3. Difference in (a) net radiation flux, (b) latent heat flux, (c) sensible heat flux, and (d) ground heat flux at the soil surface between using $C_k = 8$ and $C_k = 0$ in the frozen soil model at Rosemount station from 1 to 21 Nov 1996 (W m^{-2}).

content at all observational depths. The MBEs for soil temperature at different depths are all less than 0.3°C, and the maximal RMSE of 2.18°C appears in the surface layer. The possible causes for a relatively high RMSE for soil temperature in the surface layer is likely due to the estimations of precipitation and downward longwave radiation. Based on the change in observational soil water contents and water balance, we speculated that at least a small precipitation event (about 2–3 mm) occurred at the D66 site during this simulation period. This speculation seems to be confirmed by the simulation results. When we added this amount of the precipitation as a forcing, the simulation results improved. However, this adjustment does not solve all the problems because it is apparently a rough estimation. The largest absolute MBE of 0.03 and RMSE of 0.05 for volumetric liquid water content appear in the soil layer at 4-cm depth, while the observation for water content in the surface layer was not conducted. The downward longwave radiation flux, as the main energy source during the winter season (Yang et al. 1997), was not observed but calculated based on Kondo and Xu's (1997) scheme. Table 4 and Fig. 2 show that simulated soil temperatures and volumetric liquid water contents are in good agreement with half-hourly observed values at most depths, especially in the freezing period, and show well the advance of the freezing front toward the deep soil layers (Fig. 2). The freezing process at night and thawing process in the day in the top 20-cm soil layer are also well simulated (Fig. 2d). The smaller MBE and RMSE for soil temperature and liquid water content in the deeper soil layers indicate good model performance.

b. Sensitivity test

To investigate how the inclusion of the effect of ice content on soil matric potential could influence simulation results, a sensitivity study using the frozen soil

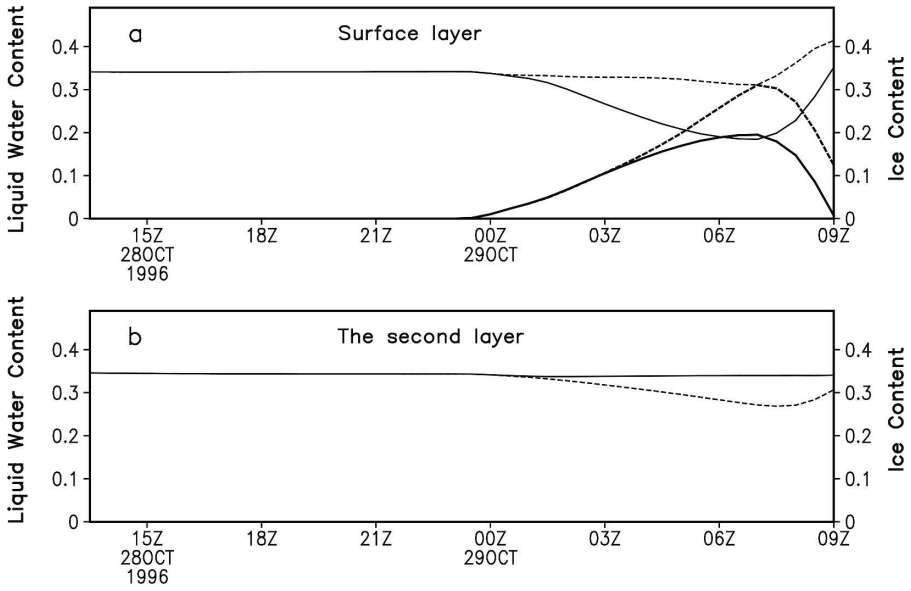

FIG. 4. (a), (b) Soil volumetric liquid water content ($m^3\ m^{-3}$) (thin lines) and ice content ($m^3\ m^{-3}$) (thick lines) simulated by the frozen soil model with (solid lines) and without (dashed lines) inclusion of the effect of ice content on hydraulic conductivity at the indicated depth at Rosemount station. (Z denotes UTC hour in the tick labels.)

parameterization scheme with $C_k = 0$ in Eq. (4) has also been conducted at Rosemount station. Simulation results show that the scheme with $C_k = 0$ underestimates unfrozen water content (with the maximal difference about 0.1) and diurnal change of soil temperature (with the maximal difference about 1°C) against the observation (not shown) and overestimates ice content. The differences in surface energy flux between simulations with $C_k = 8$ and $C_k = 0$ are presented in Fig. 3. Latent heat fluxes with $C_k = 8$ are larger than those with $C_k = 0$ and the maximum differences at midday can reach about 10 W m^{-2}. Overestimated ice content releases/absorbs more latent heat of freezing/thawing and leads to more ground heat flux into/from the atmosphere at night/in the daytime. The maximum differences in ground and sensible heat fluxes are approximately 50 W m^{-2} between the two cases, which means that the effect of ice on matric potential influences the partitioning of surface energy fluxes.

We also tested the frozen soil scheme without inclusion of the impedance of ice to soil water flow [i.e., $E_i = 0$ in Eq. (6)]. When phase changes occur in the surface soil layer, calculated upward water fluxes with $E_i = 0$ toward the freezing front are about two orders of magnitude larger than those with $E_i = 17$ due to ice's effect on hydraulic conductivity. These overestimated upward water fluxes would bring in a large amount of liquid water from the second layer to the surface soil layer, and sometimes the water content in that layer becomes unrealistically supersaturated (Fig. 4). Therefore, inclusion of the impedance of ice to soil water flow is necessary for the soil hydraulic conductivity parameterization as shown in Eqs. (6) and (7) to produce realistic results.

5. Conclusions

We present a new frozen soil parameterization that couples the water flow and heat transfer in soil with water phase change. The generalized mixed-form Richards' equation is adopted to describe soil water flow due to the matric potential gradient caused by both moisture gradient in unfrozen soil and temperature gradient in frozen soil. In addition, the effect of ice content on soil matric potential and hydraulic conductivity has been taken into account in the frozen soil hydrologic parameterization. A new modified Picard iteration method is developed to solve the fully implicit mixed-form Richards' difference equation with a phase change term, and an efficient computational scheme has been designed for the complex nonlinear equation set. Comparisons of simulation results with observational data from the Rosemount station and from the GAME/Tibet D66 site show that the frozen soil model can successfully simulate the behaviors of both the soil temperature and the water content profiles. Sensitivity experiments show that the inclusions of the effect of ice content on matric potential and the impedance of ice to

soil water flow are important for simulation of thermal and hydrological processes in frozen soil.

Acknowledgments. This work is supported by the following projects: 1) the Chinese Natural Science Foundation of China Grant 40233034, 2) the Innovation Project of the Chinese Academy of Sciences (Grant KZCX3-SW-229), and 3) the U.S. NSF Grant NSF-ATM-0353606. The authors thank Jie Song from Northern Illinois University for helpful comments; John M. Baker from the University of Minnesota and Dr. Qinyun Duan of the University of California/LLNL for providing the data from Rosemount Agricultural Experiment Station; and Mei Xue Yang from the Cold and Arid Regions Environmental and Engineering Research Institute, CAS, for providing the data from the Tibet D66 site.

REFERENCES

Beringer, J., A. H. Lynch, F. S. Chapin III, M. Mack, and G. B. Bonan, 2001: The representation of Arctic soils in the Land Surface Model: The importance of mosses. *J. Climate,* **14,** 3324–3335.

Cary, J. W., and H. F. Mayland, 1972: Salt and water movement in unsaturated frozen soil. *Soil Sci. Soc. Amer. Proc.,* **36,** 549–555.

Celia, M. A., E. T. Bouloutas, and R. L. Zarba, 1990: A general mass-conservative numerical solution for the unsaturated flow equation. *Water Resour. Res.,* **26,** 1483–1496.

Cherkauer, K. A., and D. P. Lettenmaier, 1999: Hydrologic effects of frozen soils in the upper Mississippi River basin. *J. Geophys. Res.,* **104,** 19 599–19 610.

Clapp, R. B., and G. M. Hornberger, 1978: Empirical equations for some soil hydraulic properties. *Water Resour. Res.,* **14,** 601–604.

Cox, P. M., R. A. Betts, C. B. Bunton, R. L. H. Essery, P. R. Rowntree, and J. Smith, 1999: The impact of new land surface physics on the GCM simulation of climate and climate sensitivity. *Climate Dyn.,* **15,** 183–203.

Dai, Y., and Coauthors, 2003: The Common Land Model. *Bull. Amer. Meteor. Soc.,* **84,** 1013–1023.

Farouki, O. T., 1981: The thermal properties of soil in cold regions. *Cold Reg. Sci. Technol.,* **5,** 67–75.

——, 1986: *Thermal Properties of Soils.* Series on Rock and Soil Mechanics, Vol. 11, Trans Tech Publications, 136 pp.

Flerchinger, G. N., and K. E. Saxton, 1989: Simultaneous heat and water model of a freezing snow–residue–soil system. I. Theory and development. *Trans. ASAE,* **32,** 565–571.

Fuchs, M., G. S. Campbell, and R. I. Papendick, 1978: An analysis of sensible and latent heat flow in a partially frozen unsaturated soil. *Soil Sci. Soc. Amer. J.,* **42,** 379–385.

Guymon, G. L., R. L. Berg, and T. V. Hromadka, 1993: Mathematical model of frost heave and thaw settlement in pavements. CRREL Rep. 93-2, 126 pp.

Hansson, K., J. Simunek, M. Mizoguchi, L. C. Lundin, and M. T. van Genuchten, 2004: Water flow and heat transport in frozen soil: Numerical solution and freeze/thaw applications. *Vadose Zone J.,* **3,** 693–704.

Harlan, R. L., 1973: Analysis of coupled heat-fluid transport in partially frozen soil. *Water Resour. Res.,* **9,** 1314–1323.

Huang, K., B. P. Mohanty, F. J. Leij, and M. T. van Genuchten, 1998: Solution of the nonlinear transport equation using modified Picard iteration. *Adv. Water Res.,* **21,** 237–249.

Jame, Y. W., and D. I. Norum, 1980: Heat and mass transfer in a freezing unsaturated porous medium. *Water Resour. Res.,* **117,** 811–819.

Johanson, O., 1975: Thermal conductivity of soils. Ph.D. dissertation, University of Trondheim, 236 pp.

Kondo, J., and J. Q. Xu, 1997: Seasonal variations in the heat and water balances for nonvegetated surfaces. *J. Appl. Meteor.,* **36,** 1676–1695.

Koren, V., J. Schaake, K. Mitchell, Q. Y. Duan, F. Chen, and J. M. Baker, 1999: A parameterization of snowpack and frozen ground intended for NCEP weather and climate models. *J. Geophys. Res.,* **104** (D16), 19 569–19 585.

Kulik, V. Y., 1978: *Water Infiltration into Soil* (in Russian). Gidrometeoizdat, 93 pp.

Li, X., and T. Koike, 2003: Frozen soil parameterization in SiB2 and its validation with GAME-Tibet observations. *Cold Reg. Sci. Technol.,* **36,** 165–182.

Lundin, L.-C., 1990: Hydraulic properties in an operational model of frozen soil. *J. Hydrol.,* **118,** 289–310.

Luo, L. F., and Coauthors, 2003: Effects of frozen soil on soil temperature, spring infiltration, and runoff: Results from the PILPS 2(d) experiment at Valdai, Russia. *J. Hydrometeor.,* **4,** 334–351.

Miller, R. D., 1980: Freezing phenomena in soil. *Application of Soil Physics,* D. Hillel, Ed., Academic Press, 255–299.

Mikan, C. J., J. P. Schimel, and A. P. Doyle, 2002: Temperature controls of microbial respiration above and below freezing in arctic tundra soils. *Soil Biol. Biochem.,* **34,** 1785–1795.

Mölders, N., and J. E. Walsh, 2004: Atmospheric response to soil-frost and snow in Alaska in March. *Theor. Appl. Climatol.,* **77,** 77–115.

——, U. Haferkorn, J. Döring, and G. Kramm, 2003: Long-term numerical investigations on the water budget quantities predicted by the hydro-thermodynamic soil vegetation scheme (HTSVS). Part I: Description of the model and impact of long-wave radiation, roots, snow, and soil frost. *Meteor. Atmos. Phys.,* **84,** 115–135.

Niu, G.-Y., and Z.-L. Yang, 2006: Effects of frozen soil on snowmelt runoff and soil water storage at a continental scale. *J. Hydrometeor.,* **7,** 937–952.

Pauwels, V. R. N., and E. F. Wood, 1999: A soil–vegetation–atmosphere transfer scheme for the modeling of water and energy balance processes in high latitudes. 1. Model improvements. *J. Geophys. Res.,* **104,** 27 811–27 822.

Peixoto, J., and A. H. Oort, 1992: *Physics of Climate.* American Institute of Physics, 200 pp.

Peters-Lidard, C. D., E. Blackburn, X. Liang, and E. F. Wood, 1998: The effect of soil thermal conductivity parameterization on surface energy fluxes and temperature. *J. Atmos. Sci.,* **55,** 1209–1224.

Poutou, E., G. Krinner, C. Genthon, and N. de Noblet-Ducoudré, 2004: Role of soil freezing in future boreal climate change. *Climate Dyn.,* **23,** 621–639.

Shoop, S. A., and S. R. Bigl, 1997: Moisture migration during freeze and thaw of unsaturated soils: Modeling and large scale experiments. *Cold Reg. Sci. Technol.,* **25,** 33–45.

Slater, A. G., A. J. Pitman, and C. E. Desborough, 1998: Simula-

tion of freeze-thaw cycles in a general circulation model land surface scheme. *J. Geophys. Res.,* **103,** 11 303–11 312.

Smirnova, T. G., J. M. Brown, S. G. Benjamin, and D. Kim, 2000: Parameterization of cold-season processes in the MAPS land-surface scheme. *J. Geophys. Res.,* **105** (D3), 4077–4086.

Stähli, M., P. E. Jansson, and L. C. Lundin, 1999: Soil moisture redistribution and infiltration in frozen sandy soils. *Water Resour. Res.,* **35,** 95–103.

Sun, S. F., J. M. Jin, and Y. K. Xue, 1999: A simple snow–atmosphere–soil transfer model. *J. Geophys. Res.,* **104,** 19 587–19 597.

——, X. Zhang, and G. A. Wei, 2003: A simplified version of the coupled heat and moisture transport model. *Global Planet. Change,* **37,** 265–276.

Takata, K., and M. Kimoto, 2000: A numerical study on the impact of soil freezing on the continental-scale seasonal cycle. *J. Meteor. Soc. Japan,* **78,** 199–221.

Taylor, G. S., and J. N. Luthin, 1978: A model for coupled heat and moisture transfer during soil freezing. *Can. Geotech. J.,* **15,** 548–555.

Viterbo, P., A. Beljaars, J. F. Mahfouf, and J. Teixeira, 1999: The representation of soil moisture freezing and its impact on the stable boundary layer. *Quart. J. Roy. Meteor. Soc.,* **125,** 2401–2426.

Warrach, K., H. T. Mengelkamp, and E. Raschke, 2001: Treatment of frozen soil and snow cover in the land-surface model SEWAB. *Theor. Appl. Climatol.,* **70,** 23–37.

Williams, P. J., 1967: Properties and behaviors of freezing soils. Norwegian Geotechnical Institute Publ. 72, 119 pp.

Xu, X. Z., J. C. Wang, and L. X. Zhang, 2001: *Physics of Frozen Soil* (in Chinese). Chinese Science Press, 351 pp.

Yang, M. X., T. Yao, X. Gou, T. Koike, and Y. He, 2003: The soil moisture distribution, thawing–freezing processes and their effects on the seasonal transition on the Qinghai-Xizang (Tibetan) plateau. *J. Asian Earth Sci.,* **21,** 457–465.

Yang, Z. L., R. E. Dickinson, A. Robock, and K. Y. Vinnikov, 1997: Validation of the snow submodel of the Biosphere–Atmosphere Transfer Scheme with Russian snow cover and meteorological observational data. *J. Climate,* **10,** 353–373.